Title

- T cells are necessary for development of PCOS reproductive symptoms in a letrozole-induced mouse model of PCOS
- Short T cells drive PCOS reproductive impairments

Authors

Naveena Ujagar[1], Leandro M. Velez[2,3], Gabriela De Robles[1,2], Christy Nguyen[1,2], Kiara Wiggins[1], Joshua Kim[1], Nandini Naidu[4], Julio Ayala Angulo[1], Alexander S. Kauffman[5], Varykina G. Thackray[5,6], Beata Banaszewska[7], Ewa Wysocka[7], Antoni Duleba[5], Marcus Seldin[2,3*], Dequina Nicholas[1,2,3*]

Affiliations

[1]Department of Molecular Biology and Biochemistry, School of Biological Sciences, University of California Irvine, Irvine, CA, United States.

[2]Department of Biological Chemistry, University of California Irvine, Irvine, CA, United States.

[3]Center for Epigenetics and Metabolism, University of California Irvine, Irvine, CA, United States.

[4]Department of Microbiology and Immunology, University of Reno, Reno, CA, United States.

[5]Department of Obstetrics, Gynecology, and Reproductive Sciences, University of California San Diego, La Jolla, CA, United States.

[6]Center for Obstetrics and Gynecology Research Innovation, University of California San Diego, La Jolla, CA, United States

[7]Division of Infertility and Reproductive Endocrinology, Department of Laboratory Diagnostics, Poznan University of Medical Sciences, 60-569 Poznan, Poland.

*Correspondence: dequinaa@uci.edu, Tel.: 1- 949-824-8739; mseldin@uci.edu, Tel.: 1-949-824-6765

Abstract

Polycystic ovary syndrome (PCOS) is a complex condition with clear genetic susceptibilities that impact the heterogeneous clinical presentation of symptoms and severity through unknown mechanisms. Chronic inflammation is linked to PCOS, but a clear cause-and-effect relationship has yet to be established. This study used an in depth systems immunology approach and a letrozole-induced PCOS mouse model to identify changes in inflammatory factors associated with PCOS symptoms. By analyzing immune cells and secreted cytokines from 22 different mouse strains, we identified TNF-β as a key T cell-derived cytokine associated with PCOS, regardless of genetic background. We confirmed elevated TNF-β transcripts in immune cells from women with PCOS. Importantly, we used a knockout of TCRα to show that functional T cells are a necessary component of driving PCOS features in letrozole-treated female mice. These findings implicate T cells and specifically TNF-β production in the development of PCOS impairments. T cells are therefore an attractive target for the future development of anti-inflammatory therapeutics to improve PCOS symptoms.

Teaser

TNF-β links T cell inflammation to reproductive dysfunction in PCOS, highlighting new therapeutic targets for this disorder.

MAIN TEXT

Introduction

Polycystic Ovary Syndrome (PCOS) is the most common reproductive disorder in women of childbearing age, affecting as many as 10-15% of women (1). PCOS is characterized by polycystic ovaries, oligo- or anovulation, and clinical or biochemical hyperandrogenism, which ultimately results in infertility (2). Clinically, women with PCOS present heterogeneously and PCOS is categorized as types A-D based on three primary features: hyperandrogenism, irregular cycles (an- or oligo-ovulation), and polycystic ovaries (2,3). Type A or Classic PCOS is characterized by presentation of all three primary features and is often accompanied with symptoms like hirsutism, acne, infertility, and metabolic syndrome. Type A is the most prevalent and most studied subtype of PCOS and the LET-induced mouse model of PCOS in C57BL6 mice recapitulates symptoms observed in this subtype (4). Women with Type B or non-PCOM PCOS have hyperandrogenism and irregular cycles but no polycystic ovaries. Type C or Ovulatory PCOS presents with hyperandrogenism and polycystic ovaries but regular ovulation. Finally, Type D or non-androgenic PCOS is characterized by ovulatory dysfunction and polycystic ovaries without elevated levels of androgen.

PCOS patients also exhibit chronic low grade inflammation. In particular, C reactive protein (CRP), a broad indicator of inflammation, is 96% higher in women with PCOS than those without (5). Currently, CRP is the most reliable marker of chronic inflammation in PCOS (5,6). Across studies, CRP is consistently upregulated in women with PCOS (5–7). However, the literature is filled with conflicting results on mediators of this chronic inflammation. Despite consistency in elevated CRP, no differences in circulating cytokines, such as IL-6, were detected in women with and without PCOS in several cohorts, though this was likely a consequence of small sample size (8–10). However, a meta-analysis of BMI-matched cohorts revealed significantly increased IL-6 in women with PCOS that correlated with insulin resistance (11). The latter outcome is supported by a report demonstrating that administration of exogenous androgen to healthy women to an elevated level observed in PCOS increases circulating IL-6 (12). Clinical studies have begun to define inflammation in PCOS by identifying increased circulating levels of IL-1α, IL-1β, TSP-1 and TGF-β1 in PCOS (13,14). Additionally, circulating neopterin (a protein made by macrophages) is elevated in PCOS independent of BMI (15). TNF-β, a T cell derived cytokine, was found to be increased in serum of women with PCOS no matter their BMI status (16). Collectively, the clinical literature provides emerging evidence of exacerbated chronic inflammation in PCOS but fails to inform on the source of that inflammation, whether the inflammation drives any PCOS symptomology, and what are the specific factors involved, questions better addressed using a pre-clinical animal model.

Kauffman et al. developed a mouse model that utilizes chronic treatment with letrozole (LET), a nonsteroidal aromatase inhibitor, initiated in peri-pubertal life to induce the reproductive and metabolic hallmarks of PCOS in C57BL6 mice (4). The LET mouse model recapitulates the Type A subtype of PCOS. Aromatase inhibition prevents the conversion of androgens to estrogens,

thereby resulting in elevated circulating androgen levels that mimic the hyperandrogenism observed in PCOS patients. In addition to eliciting high androgen levels, the LET PCOS-like mouse model is particularly effective in inducing other critical features of the disorder, including irregular estrous cycles, polycystic ovaries, anovulation, and metabolic dysfunction such as insulin resistance and body weight gain (4,17). Generally accepted relevant for PCOS research, the LET model exhibits at least two characteristics that are comparable to the Rotterdam criteria used to diagnose PCOS in women (18). This model also successfully recapitulates underlying endocrine mechanisms observed in women with PCOS, such as abnormally increased, hyperactive luteinizing hormone (LH) pulse (19)(20).

Recent studies have highlighted the complex interplay between genetic predisposition and environmental factors in shaping the diversity of PCOS phenotypes. For instance, a genome-wide association study by Day et al. identified 14 novel loci associated with PCOS, suggesting a strong genetic component to the syndrome (21). However, the expression of these genetic variants can be significantly influenced by environmental factors. Lifestyle factors such as diet and exercise have been shown to modulate PCOS symptoms. For example, weight loss through lifestyle intervention can improve metabolic and reproductive outcomes in women with PCOS, regardless of their genetic predisposition, implicating conserve mechanisms (22). Furthermore, epigenetic modifications, which can be influenced by both genetic and environmental factors, have been implicated in PCOS pathogenesis. Kokosar et al. identified altered DNA methylation patterns in adipose tissue of women with PCOS, suggesting that epigenetic changes may contribute to the metabolic dysfunction often observed in the syndrome (23). These findings underscore the importance of considering both genetic and environmental factors when studying PCOS phenotypes to decipher mechanism specific to disease development.

The high variability and severity of PCOS phenotypes across women with the disorder poses challenges in identifying inflammation-related mechanisms specific to PCOS. Using the LET-induced model of PCOS and a genetic screen, we aimed to address the challenge of identifying immune mediators specific to PCOS and the relationship of those immune mediators diverse PCOS phenotypes. Here, we perform a comprehensive and robust analysis of immune cells and cytokines associated with PCOS symptoms. Using a systems genetics approach by analyzing placebo and LET treated female mice across 22 distinct inbred mouse strains, we 1) are able to recapitulate the diversity of phenotypic outcomes observed in women with PCOS, 2) identify T cell associated cytokines, specifically TNF-β, as candidate immune drivers of reproductive dysfunction in PCOS-like conditions, and 3) identify a novel requirement for functional T cell action in the induction of PCOS-like impairments.

Results

Confirmation of PCOS-like symptoms in LET-induced mouse model in multiple genetic strains

To determine the inflammatory response characteristics in a PCOS-like condition, we implanted LET or placebo (control) pellets in 130 young adult female mice across 22 diverse inbred strains. Pellets were implanted at ~10 weeks of age and replaced with a fresh pellet after 3 weeks to ensure continuous delivery through the entire 6 week paradigm (**Figure 1A**). First, we analyzed the entire cohort to confirm the *global* induction of PCOS-like symptoms by LET treatment in these strains. As expected, compared to placebo control, LET significantly increased body weight (BW) gain over time, with a slight temporary plateau due to recovery from the week 3 re-implantation surgery (**Figure 1B**). LET mice gained on average 2-fold more BW than placebo control females and had significantly increased total fat (**Figure 1C and D**), confirming prior

reports (4,17,24). This increase in BW was accompanied by impaired glucose tolerance, a common metabolic symptom of PCOS (**Figure 1E and 1F).** Blood serum testosterone, of which elevated levels are often a primary diagnostic criterion for PCOS, were also significantly increased in LET mice compared to controls, mimicking hyperandrogenism in PCOS women (**Figure 1G**). LH was significantly increased as previously reported (4)(**Figure 1H**). The LH to FSH ratio, though not statistically significant, displayed a trend towards an increase in LET mice, as occurs in many women with PCOS (**Figure 1I**). Finally, the ovaries of LET mice had a significant increase in follicular cysts and fewer corpus luteum (an indicator of ovulation), consistent with PCOS ovarian morphology in women (**Figure 1J, 1K**). These data indicate that we effectively induced PCOS-like symptoms in a genetically diverse mouse cohort.

LET-induced PCOS impacts immune cell cytokine secretion but causes minimal shifts in immune cell populations

With the induction of PCOS-like phenotypes confirmed, we performed a comprehensive immunophenotyping of mouse spleen and inguinal lymph nodes in LET and control mice. We cultured dissociated spleen in the presence of anti CD3/CD28 (T cell stimuli) or Lipopolysaccharide (LPS, myeloid cell stimuli which targets Toll Like Receptor 4, TLR4) and the conditioned media was analyzed for 40 secreted cytokines (**Figure 2A**). Cells from both spleen and lymph nodes were stained with an 18 color antibody panel and analyzed by flow cytometry (**Supplemental Figure 1**). We analyzed the spleen derived cytokine profiles from adult C57BL6 mice treated with chronic LET initiated prepubertally (4), which have the classic Type A PCOS reproductive and metabolic phenotypes, and found that LET-induced PCOS females could be differentiated from control females by their cytokine profiles (**Figure 2B**). Using partial least squares discriminant analysis, a supervised clustering approach (25), we analyzed the cytokines that contributed to distinguishing these two groups. Irrespective of immune stimulation, the control group was characterized by the chemokines IP-10 and MIP1 (**Supplemental Figure 2A and B**). Overall, immune cells from the spleen of LET females were hyporesponsive to stimulation, consistent with the literature of testosterone being inhibitory to immune function (26). To determine whether the ability for cytokine profiles to discriminate placebo from LET-induced PCOS was due to broad changes in immune cell populations, we used flow cytometry to enumerate cell populations. We found virtually no significant changes in immune cell distribution in the spleen in LET mice (**Supplemental Figure 2C**). Together, these data indicate that, at least on the commonly-used C57BL6 background, changes in cytokine profiles in the LET model of PCOS are driven by functional changes rather than broad changes in immune cell distribution.

Genetic background dictates LET induced cytokine secretion in stimulate immune cells

After confirming above that LET PCOS-like mice can be distinguished from control mice by their splenic-derived cytokine profile in the C57BL6 strain (**Figure 2B and C**), we extended this analysis to a larger cohort of 22 genetic mouse strains. Unexpectedly, we were unable to construct a PLSDA model with a classification error rate above 70% from secreted cytokines, indicating that the cytokine profile could not be used to categorize disease state when analyzing the entire genetically diverse cohort (**Figure 2D and E**). Similar to the C57BL6, the distribution of immune cell populations in inguinal lymph nodes or spleen did not shift with LET-induction of PCOS symptoms (**Figure 2F and Supplemental Figure 2D**). However, after performing principle component analysis (PCA) on immune frequencies and recoloring by sample source, it was clear that variability within the dataset was driven by tissue type (**Supplemental Figure 2D**), consistent with different strains and tissues having defined frequencies of immune cell types.

These findings prompted us to desegregate the data by genetic strain and to ask whether the initial immune landscape dictated by genetic background impacted our ability to distinguish between placebo and LET mice by cytokine profiles. We therefore analyzed cytokine profiles by strain after 40 hrs of either anti-CD3/CD28 or LPS (**Figure 3A and B**). Using PLSDA, we found that within many strains, the control and LET mice clustered together. In contrast, several strains displayed divergent cytokine profiles upon LET treatment. For example, in LPS stimulated splenocytes, BxD73 and NOD strains had cytokine profiles that result in their placebo data point being located far from the centrality of the cluster for controls (**Figure 3A**). Further, cytokine profiles did not shift for BALBc/j in response to LET. However, LPS-induced cytokine profiles from DBA mice displayed a clear shift (**Figure 3B**). These data show that genetic background is important for the magnitude of the inflammatory response to LET treatment.

Memory CD4 T cell frequencies are associated with LET treatment

Genetic strain alone substantially impacts the basal immune cell distribution of immune cells in the spleen (27). When we compared the DBA strain (common strain with large immune shift with LET treatment) to the BABLc/j strain (common strain with negligible immune shift with LET treatment), we found that their basal immune cell composition was completely different (**Figure 3C and D**). Immune frequencies of these two strains were easily separated on PC1. To determine what features were responsible for this separation, we performed K means clustering projected onto a PCA plot (**Figure 3D**). The DBA strain was B cell skewed while BALBc/j mice were skewed toward CD4+ and CD8+ T cells, with both strains sharing features of naive CD4+ T cells. LET-treatment in either of these strains had no impact on the baseline immune cell composition (**Supplemental Figure 3**). Given that genetic strain appeared to dictate immune cell composition, we performed a formal heritability estimate analysis using a linear mixed effects model across all of the strains and two treatment groups to determine which cell populations are explained by genetics, LET treatment, or both (**Figure 3E and F**). In the inguinal lymph nodes, we found that ~50% of immune cell composition is explained by genetic strain (**Figure 3E**). In the spleen, which is representative of systemic immune function, we see that LET treatment alone explains ~20% of the variance in memory CD4+ T cells. These memory CD4+ T cells are the immune subset with the largest proportion of significance explained by LET treatment alone. Collectively, these data indicate that the immune variability introduced by the genetic diversity supersedes the immune variability induced by LET treatment. Despite the high variation in baseline immune composition and cytokine secretion, heritability estimates identified memory CD4+ T cells in spleen, along with myeloid cells and dendritic cells, as modulated by LET treatment.

T cell derived cytokines correlate with metabolic and reproductive measures of PCOS

The large genetic diversity of this study provides variation and robust statistical power to identify novel relationships between immune variables and phenotypic outcomes. Given that cytokine profiles show modulation by LET treatment by strain, we performed multiple correlation analysis using reproductive and metabolic outcomes associated with PCOS and cytokines measured from T cell or LPS stimulated immune cells from these mice (**Figure 4**). To identify strong cytokine signatures associated with reproductive or metabolic PCOS outcomes, we focused on correlation patterns that were conserved within treatment groups regardless of immune stimuli. In control mice, MCP-1 and other inflammatory cytokines known to be associated with ovarian tissue remodeling were positively correlated with follicular cysts. This relationship, likely indicative of homeostatic mechanisms, was not present in PCOS-like mice. Interestingly, we observed that a subset of T cell cytokines (IL-33, IL-17E, CD40LG, IL-27, and TNF-β) were positively correlated with lean/fat ratio in either T cell or myeloid stimulation conditions. Of note, TNF-β, recently

discovered to be elevated in women with PCOS (16), was not detectable from T cell stimulated control cells. We also performed correlative analysis of immune cell frequencies to reproductive and metabolic outcomes in our cohort and identified significant correlations including CD4 T cells with insulin, B cells with glucose tolerance, and CD8 T cells with lean fat ratio (**Supplemental Figure 4**). Together, these data suggest that immune function in LET mice is correlated to PCOS phenotypes.

T cell derived cytokines, especially TNF-β, are potential immune targets in PCOS

Given the large genetic variability across our 22 strain cohort, we asked whether LET-induced phenotypes in some strains might represent additional clinical subtypes of PCOS. For every strain, we compared LET to their matched control and determined whether exhibited hyperandrogenism (elevated serum T), impaired estrous cyclicity, an- or oligo-ovulation (reduced corpora lutea), and polycystic ovarian morphology as determined by number of cysts per ovary (**Table 1**). We next asked the question of whether cytokine profiles could discriminate between PCOS that presented with or without a metabolic phenotype using PLSDA (**Figure 5 and Supplemental Figure 5**). We compared strains with high metabolic dysfunction to strains with low metabolic dysfunction to mirror the approach of comparing genetic signatures of women that do or no not develop metabolic dysfunction with PCOS (28). With T cell stimulation (**Supplemental Figure 5A**), we were able to clearly differentiate high metabolic dysfunction phenotypes from low metabolic dysfunction. When we analyzed the loadings for the these PLSDA plots (**Figure 5A and B**), a consistent group of cytokines was implicated in metabolic dysfunction. Heritability estimates for cytokines across all strains determined that some cytokines were strain independent, with variability only explained by LET treatment or the interaction of LET with the genetic background (**Figure 5C and D**). Several of these cytokines, including TNF-β, IL-17F, and IL-25, were also discriminators for metabolic dysfunction (**Figure 5A and B**) or correlated with PCOS phenotypic measurements (**Figure 4**).

We next tested whether these identified T cell derived cytokines were increased in human PCOS. Peripheral blood mononuclear cells (PBMCs) from a cohort of adult women with (n=15) and without (n=5) PCOS were analyzed (**Table 2, Figure 6A**). As expected, women with PCOS had elevated testosterone (**Table 2, Supplemental Figure 6**), fewer menses per year , more acne, and larger ovarian volume compared to controls (**Table 2**). This cohort of women with PCOS did not have a strong metabolic phenotype, and there were no significant group differences in insulin response or GTT (**Table 2**, **Figure 6B-D**), though the lipid profiles of these women with PCOS were characterized by higher triglyceride levels and lower HDL cholesterol (**Figure 6E-H**). From the PBMCs of this cohort, we extracted mRNA and performed qPCR for IL-25, IL-9, IL-27, CD40LG, IL-33, TNF-β, and IL-1A. Of the 3 cytokine transcripts that were detectable, only TNF-β mRNA (*LTA*) was significantly increased in women with PCOS (**Figure 6I**), indicating that T cell-derived cytokines, specifically TNF-β, are associated with PCOS in women.

TNF-β expression in human spleen is correlated with adipose expression of LPS inducible genes

Given that spleen was the source of TNF-β from which we discovered the correlations with PCOS like symptoms in mice, we determined whether similar correlations existed within human datasets. To bridge the gap between measuring *LTA* (the gene for TNF-β) in PBMCs and not from spleen, we analyzed and integrated data from the Genotype-Tissue Expression (GTEx) project (29). GTEx is a well-powered bulk transcriptomic research initiative aimed at understanding the relationship between genetic variation and gene expression across different human tissues. From GTEx, we sampled bulk transcriptomic data from premenopausal women (n=31, age <50), and

determined the co-correlation of spleen *LTA* expression with gene expression in other tissues (**Figure 7A**). We found that adipose had the most genes which correlated with spleen LTA. We next performed pathway analysis on *LTA*-correlated adipose genes and discovered strong signatures for leukocyte chemotaxis and an LPS response. We conclude that splenic expression of LTA correlates with adipose expression of inflammatory genes.

The reproductive phenotype of PCOS is dependent on T cells

LTA is expressed and highly inducible in both B and T cells. However, given our T cell data and a prior report that knockout of B cells in a PCOS-like model did not alter disease (30), we tested whether T cells are necessary for development of PCOS phenotypes by utilizing the LET paradigm in young adult TCRα KO mice and several WT controls. TCRα KO mice generate T cells but do not have a functional αβ T cell receptor, and therefore their T cells do not become activated. Outcomes from the present TCRαKO cohort were compared to our previously published cohort of adult C5BL6 mice (31). When LET is introduced in C57BL6 mice in adulthood as opposed to peri-pubertally, WT mice have a weak metabolic phenotype but a strong reproductive phenotype (24). As expected, the control WT mice treated with LET had a strong reproductive phenotype which matched our published cohort including extended time spent in diestrus and elevated LH (**Figure 8A and B, Supplemental Figure 7)**, similar to our human cohort (**Table 2, Figure 6)**. Like WT C7BL6 mice, TCRα KO mice treated with LET did not have a metabolic phenotype compared to placebo (**Supplemental Figure 7A-C**). In contrast to LET WT, TCRα KO mice treated with LET were protected from the development of PCOS-like reproductive impairments (**Figure 8A and B, Supplemental Figure 7D, G and H**). LET TCRα KO mice were not arrested in diestrus in contrast to LET WT mice that were acyclic and in diestrus (**Supplemental Figure 7D, G and H**). Lack of functional T cells had no impact on LET-induced elevation of testosterone (Figure 8A), but was protective for the PCOS associated increase in LH (**Figure 8B**). When we analyzed the cytokine profiles derived from the spleens of these mice, we confirmed, as in Figure 2, that the immune cells are generally hyporesponsive in the control LET-treated C57BL6 mouse compared to Placebo (**Figure 8F and G**). Unlike in Figure 2 which demonstrated that Placebo vs LET mice could be clearly identified by their LPS induced cytokine profiles, we were unable to distinguish between Placebo and LET LPS-induced cytokine profiles in the TCRα KO mice. These data suggest that T cells and T cell-derived cytokines are necessary for the induction of some PCOS-like reproductive symptoms (cycles, LH levels), at least in the LET model.

Discussion

In this study, we demonstrate using a systems genetics screen that variation in T cell derived cytokines, specifically TNF-β, is LET treatment specific. By knocking out functional T cells, a major source of TNF-β, we provide evidence for T cells being necessary for the development of PCOS reproductive symptoms. The major findings of this study have broad implications for the treatment of PCOS.

First, we demonstrate that by varying genetic background, we can recapitulate broader presentations of PCOS phenotypes. Several BxD strains including 124,129, and 60 in addition to the CH3/Hej, DBA, and NOD strains developed symptoms similar to PCOS type A, the most common amongst the mouse strains (32). A/j and BxD125 responded to LET treatment with symptoms similar to type B PCOS while two BxD strains (48 and79) responded to LET treatment similar to symptoms of PCOS type C. BxD77 was the only strain that resembled a type D phenotypic presentation of PCOS in response to LET treatment. The ability to generate this

diversity of phenotypes in response to LET treatment increases the ability to discover genetic based mechanisms for PCOS phenotypes. There are several animal models of PCOS including the pre-pubertal and adult LET paradigms used in this study. Other models include the administration of dihydrotestosterone (DHT, a non-aromatizable androgen), perinatal and prepubetal exposure to anti-Mullerian Hormone (AMH) among others (reviewed in (33)). These models have varied presentation of PCOS phenotypes and now by using a genetic diversity panel, we can capture this same type of diversity using a single paradigm.

Our analysis of PCOS phenotypes with or without metabolic dysregulation suggests that the underlying immune function amongst these phenotypes may be different and thus may require developing separate approaches to anti-inflammatory treatments. The same was not true for LPS-induced cytokine profiles indicating that T cell derived cytokines are equally important for reproductive outcomes but a subset of specific cytokines likely play a role in driving metabolic dysfunction.

The finding that TNF-β was altered in PCOS suggests that it could be a potential target for treatment in PCOS. We found that gene expression of TNF-β correlated with changes in gene signatures in the adipose. Specifically, *LTA* expression in the spleen correlated with adipose gene signatures for leukocyte chemotaxis and an LPS response. Taken together with published data demonstrating increased circulating TNF-β in women with PCOS (16), our findings implicate TNFβ as a potential regulator of LPS-induced adipose inflammation and metabolic dysfunction in PCOS. There is strong precedent that targeting immune dysfunction is beneficial for PCOS. For example, women with PCOS who take metformin, known to have anti-inflammatory properties in addition to reducing hepatic gluconeogenesis, experience improvement of ovulatory function (34–36). This effect of metformin implies that blocking chronic inflammation ameliorates the reproductive phenotypes of PCOS. Given there has been no explicit target for inflammation in PCOS, clinical trials directly testing immune therapy for improvement of PCOS symptoms has not been justified. Our study provides a foundation for targeting T cells in PCOS and more specifically TNF-β, which we demonstrated correlates with adipose inflammatory gene expression in humans.

The most striking finding in our study was that increased LH and downstream reproductive function in the LET mouse model was not observed in TCRα KO mice despite increased testosterone. This data indicates that T cells may be necessary for development of PCOS and highlights the potential of T cells to drive reproductive phenotypes in the absence of hyperandrogenism, a hypothesis which needs to be empirically tested. In the absence of high LH, it is likely that local mechanisms in the ovaries are supporting high testosterone. It is possible that in PCOS, testosterone feedback to reduce LH production is nonfunctional. T cells may be the disruptors of this feedback mechanism. If T cells do indeed disrupt testosterone feedback, then our data demonstrate that a lack of T cells keeps negative feedback inhibition intact, thereby resulting in high testosterone through the inhibition aromatase and low LH because of negative feedback. Adoptive transfer of memory T cells from LET female mice to control mice would answer whether T cells break testosterone negative feedback.

Despite the clear findings of our study, limitations remain. The study is underpowered to dissect strain specific outcomes. We opted for increased genetic diversity with the goal to use the variation to identify inflammatory mediators that are specific to PCOS as opposed to what may be different on a strain-by-strain basis. Additionally, we derive cytokine profiles from stimulation of splenic immune cells rather than assessing circulating cytokines in serum. This approach results in reproducible and controlled cytokine profiles with reduced variability compared to serum

cytokine profiles. Further, the concentration of cytokines in mouse serum is considerably lower than that in human and difficult to detect by Luminex, thereby limiting how many targets were profiled. This being said, spleen-derived cytokine profiles may not be directly comparable to human PMBC- or serum-derived cytokine profiles, making translation of these signatures difficult. In future studies, it will be important to perform comprehensive cytokine profiles from PBMCs and serum of women with and without PCOS across all subtypes. This will confirm which cytokines, specifically TNF-β, are PCOS specific to bolster the support for developing it as a therapeutic target.

A caveat of this study is our use of the adult LET-induced model of PCOS symptoms as opposed to the pre-pubertal model. The age at which we receive mice to perform genetic screens was constrained by the breeding of enough matched cohorts for surgeries. As described, the C57BL6 mouse does not develop a strong metabolic phenotype when LET is introduced in adulthood (24). For this reason, we were unable to determine the impact of TCRαKO on the metabolic phenotype of PCOS. We hypothesize that TCRαKO mice may also be protected from metabolic dysfunction if subjected to the peri-pubertal LET paradigm.

Before this work can be translated into a feasible treatment for PCOS, there are several questions that remain to be answered. First, we must determine which T cells are mediating the PCOS phenotypes. We removed the function of all αβT cells. Therefore, it would be important to determine if the LET-induced symptoms were dependent on CD4 or CD8, and if CD4 then what type. If a particular subset of CD4 T cells, such as Th1, Th2, Th17 or Treg are driving disease, then targeting T cells as an intervention could be more specific. Our cytokine profiling across several figures of our study implicates a potential Th17 mechanism that would need to be confirmed, consistent with Th17 inflammation driving metabolic dysfunction (37–39). Finally, to truly translate this work to the clinic, intervention studies need to be performed across different strains representing all four subtypes of PCOS. These pre-clinical studies would include depleting T cells or neutralizing TNF-β after development of symptoms in the LET model. These approaches would confirm the feasibility of targeting T cells and their cytokines for immunotherapy.

Materials and Methods

Animals

All experiments adhered to the Institutional Animal Care and Use Committee (IACUC) guidelines at the University of California, Irvine and the University of California, San Diego. Female inbred and TCR alpha KO strains were acquired from Jackson Laboratories, and BxD strains were provided by Robert W. Williams and David G. Ashbrook (**Supplemental Table 1**). Mice were maintained under a 12-hour light/dark cycle with ad libitum access to food. Our PCOS model was established using a protocol adapted from prior studies (Kauffman et al., 2015; Torres et al., 2019). Female mice, aged 8-12 weeks, received subcutaneous implants of letrozole (PCOS) or placebo pellets (3mm diameter; Innovative Research of America) at the start and after 3 weeks, ensuring a continuous release of 50 μg/day of letrozole over 6 weeks. Letrozole-treated and control mice were housed separately, with no more than four mice per cage. For TCR alpha KO mice, Placebo and LET pellets were inserted at 9 weeks of age as illustrated in Figure 1. Two wildtype sentinel mice were included with the cohort to ensure the current batch of LET pellets were inducing PCOS-like symptoms. The mice underwent routine body composition analysis, echocardiography, glucose tolerance tests, estrous cycle assessments, and weekly weight measurements. At the study's conclusion, mice were euthanized using 2.5% isoflurane delivered via a precision vaporizer, followed by physical euthanasia methods. Metabolic and reproductive tissues were collected, immediately frozen in dry ice, and stored at −80°C. One ovary per mouse

was fixed in 4% paraformaldehyde at 4°C overnight, preserved in 70% ethanol, and processed for histology. Serum was collected after coagulation at room temperature for 1 h (2,000 x g for 10 min at 4°C) and stored at -80°C for subsequent analyses.

Human peripheral blood mononuclear cells

Human peripheral blood was collected from Dr. Beata Banaszewska's patient list of women with PCOS (n=15) or without PCOS (n=5). Dr. Beata Banaszewska carried out all clinical diagnostics and measurements of her patients. Peripheral blood mononuclear cells were isolated using a density gradient media and cryopreserved and shipped overnight in dry ice from Poznan University of Medical Sciences, Poland to the University of California, Irvine- where they were stored in liquid nitrogen for downstream application.

Body weight, body composition, and glucose tolerance test

Body weights were measured at the beginning of each week, and body composition measurements were taken using the EchoMRI™ Whole Body Composition Analyzer on the 5th week of the protocol. Intraperitoneal (ip) glucose tolerance tests (GTT) were performed on the 5th week in a conscious state. Briefly, mice fasted for 6 h were ip injected with 1 g of glucose/kg body mass, and glucose levels were determined from the tail-tip using a hand-held glucometer (Accu-Check Guide) in the basal state and 15, 30-, 45-, 60-, and 90-min following glucose administration.

Estrous Cycle Assessment

Owing to the number of in vivo assessments carried out on the mice, and to reduce stress on the animals, only one estrous cycle (up to 5 days) was assessed during the final week of the protocol (6th week), which allowed us to determine if the last cycle was normal (normal progression diestrus-proestrus-estrus-meta estrus) or not (arrested cycle). The estrous cycle stage was determined by light microscopic analysis of smears from the vaginal lavage. Proestrus was defined by the presence of mostly nucleated and some cornified endothelial cells, estrus as mostly cornified cells, metestrus as some cornified endothelial cells and mostly leukocytes, and diestrus as primarily leukocytes.

Ovarian morphology

To roughly estimate ovarian follicular populations, partial follicular counting and classification were performed (approximately ¼ per ovary per mouse) in ovarian serial sections (5 um/section). In brief, fixed ovarian tissue was consecutively cut, placed on gelatin-coated slides (Biobond, British Biocell International, Cardiff, UK), air dried for 2 h, and fixed for 5 min in acetone at 4 C. Subsequently, consecutive sections from each ovary were washed in PBS (137 mmol/l NaCl, 2.7 mmol/l KCl, 4.3 mmol/l Na2 HPO4.7H2O, 1.4 mmol/l KH2PO4, and pH 7.3) and stained with hematoxylin and eosin (DAKO Corporation, Carpinteria, CA, USA) for histological analysis. Histological serial sections were independently analyzed by three of the authors, and ovarian follicles were classified and quantified. The number of follicles was counted at a regular interval, and the total number of follicles per ovary was estimated using a multiplication factor based on follicle class and sampling fraction (https://doi.org/10.1186%2F1477-7827-1-11). Primordial, primary, secondary, and antral follicles were counted and classified as described previously (40). Then, follicles were grouped into primordial, small follicles (grouping primary, secondary, and small antral follicles), and large follicles (Graafian/preovulatory follicles). Follicular atresia was also quantified, and atretic follicles were defined as follicles with >5% of the granulosa cells having pyknotic nuclei.

Serum terminal assays of hormonal levels

Serum hormonal levels of luteinizing hormone (LH) (UVA in house protocol, sensitivity 0.016 ng/mL, range 0.016-4 ng/mL), follicle-stimulating hormone (FSH) (UVA in house protocol, sensitivity 0.016 ng/mL, range 0.016-8 ng/mL), estradiol (E) (Alpco, 55-ESTRT-E01, sensitivity 2.5pg/mL, range 5-1280 pg/mL), and testosterone (T) (ILB, IB79174, sensitivity 0.006 ng/mL, range 0.1-25 ng/mL) (**Figure 1**) were assessed by The University of Virginia (UVA) Center for Research in Reproduction Ligand Assay and Analysis Core. Insulin levels in serum were measured with the Mouse Insulin ELISA (Alpco, catalog 80-INSMS-E01). Alternatively, serum testosterone (**Figure 8**) was measured via the Multi-Species Hormone kit (MSHMAG-21K) and testosterone flexing pack (SPRCA1825). The Testosterone capture antibody has 100% reactivity to Testosterone and 16% cross-reactivity to 5-alpha-DHT. Briefly, 100 µL of serum was vortexed with 150 µL acetonitrile and incubated for 10 minutes at room temperature. The sample was then vortexed again for 5 seconds, then centrifuged at 17,000 x g for 5 minutes. 200 µL of supernatant was transferred into new Eppendorf tubes. The samples were dried by Speed Vac, followed by reconstitution with 80 µL Luminex Assay Buffer before being analyzed by multiplex assay. Per manufacturer's instructions, data is analyzed and presented as Mean Fluorescence Intensity (MFI).

Variance partitioning analyses (heritability)

Mixed effect models were used to estimate genetic and PCOS contributions to traits, as shown previously (41). In brief, variances were partitioned using a linear random slope model (nlme R Package) with treatment and strain as random effects. The proportion of the total variance explained by strain was scaled to explain a portion of the residual variance from the previous model as a strain-by-diet interaction. Linear modeling was performed using lme functions from the R package lme4 version 1.1-25. Variance plots were generated using the R package ggplot2 version 3.3.2.

Splenocyte stimulation and cytokine multiplex immunoassay

At the end of the 6-week treatment, the spleen of the mice was collected. The spleen cells were mechanically dissociated and stimulated (200,000 cells/200 mL) with either mouse T-activator CD3/CD28 dynabeads (1 bead per cell; ThermoFisher) or lipopolysaccharide O111:B4 (conc.; Ebioscience) for 40 hours at 37°C. The conditioned media from the stimulated splenocytes for each mouse were collected and stored at -20°C. A total of 40 cytokines and chemokines were quantified using the Milliplex MAP mouse Th17 magnetic bead panel and the Milliplex MAP mouse cytokine/chemokine magnetic bead panel (Millipore Sigma) according to the protocol from each respective kit. The analyte concentrations were measured using an Intelliflex instrument (Luminex) and the Belysa software (1.2). Two separate datasets of cytokine quantifications were generated based on whether the supernatant originated from splenocytes activated with either CD3/28 dynabeads or LPS.

Staining and Flow Cytometry

All mice inguinal lymph nodes were enzymatically dissociated using 0.25% collagenase for 30 minutes, inhibited with 0.5M EDTA and then mechanically dissociated using a 50µM strainer washed with FACS buffer. While mice spleens were mechanically dissociated using a 50uM strainer and incubated with red blood cell lysis for 5 minutes before being washed with FACS buffer. Cells were aliquoted into 96-well plates for the staining of the 18 markers (**Supplemental Table 2**) and flow cytometry was performed on Cytek Northern Lights Spectral Cytometer.

RNA isolation, reverse transcription and quantitative polymerase chain reaction

Cryopreserved peripheral blood mononuclear cells from women with PCOS (n = 15) or without PCOS (n = 5) were thawed in a 37°C water bath and washed with 10mL of RPMI 1640 media supplemented with 10% FBS. Cells underwent RNA isolation via Invitrogen's TRIzol Reagent protocol (CAT #15596018). Complementary DNA was made by reverse transcription of 2 µg total RNA using Applied Biosystems's High-Capacity cDNA Reverse Transcription Kit and protocol (CAT #4368814). Complementary DNA products were detected using iQ SYBR Green Supermix (Bio-Rad Laboratories) on a CFX Opus 384 Real-Time PCR System. Data were analyzed by the 2ΔΔCt method by normalizing genes of interest (shown below) to *Gapdh*. Primers for genes of interest were designed using NCBI's BLAST and Primer Designing Tool.

Gene symbol	Primer (5'- 3')	Reverse Primer (5'- 3')
Cd40lg	AAACCTTGCGGGCAACAATC	TGACAAACACCGAAGCACCT
Il27	CAGGCGACCTTGGCTGG	GCTGACTGTGAACTCCCTCC
Lta	CATCCCCCACCTAGTCCTCA	TGGTGACGACCCCTGAAATG

Partial least squares modeling and principal component analysis

Partial least squares discriminate analysis (PLS-DA) and principal component analysis (PCA) was done for the two datasets of cytokine and flow cytometry quantifications separately using Solo (Eigenvector Research, Inc.). Measurements were assigned as the independent variable, while the discrete regression variable was the treatment classification (LET or control), subphenotyping (A, B, C or D), or metabolic dysfunction (high or low). Two primary latent variables, LV1 and LV2, were used in leave-one-out cross-validation (n=<20) or venetian blinds (n>20). The model was deemed significant in ability to classify with an error rate greater than 70%.

Statistical analysis

All the statistical tests were performed in R (4.2.3) and PRISM GraphPad (9.5.1). In comparisons between the LET and control mice groups, Student t-tests were performed. To compare population percentages, z-tests were performed. All statistical analysis results with a p-value≤0.05 were determined as significant.

Data and Code Availability

A detailed walk-through, all scripts used for analysis, and all processed data have been made freely available at: https://github.com/Leandromvelez/Systems_genetics_PCOS

References

1. Bozdag G, Mumusoglu S, Zengin D, Karabulut E, Yildiz BO. The prevalence and phenotypic features of polycystic ovary syndrome: a systematic review and meta-analysis. Hum Reprod. 2016 Dec;31(12):2841–55.

2. Christ JP, Cedars MI. Current Guidelines for Diagnosing PCOS. Diagnostics (Basel). 2023 Mar 15;13(6):1113.

3. Unfer V, Kandaraki E, Pkhaladze L, Roseff S, Vazquez-Levin MH, Laganà AS, et al. When one size does not fit all: Reconsidering PCOS etiology, diagnosis, clinical subgroups, and subgroup-specific treatments. Endocrine and Metabolic Science. 2024 Mar 31;14:100159.

4. Kauffman AS, Thackray VG, Ryan GE, Tolson KP, Glidewell-Kenney CA, Semaan SJ, et al. A Novel Letrozole Model Recapitulates Both the Reproductive and Metabolic Phenotypes of Polycystic Ovary Syndrome in Female Mice. Biol Reprod. 2015 Sep;93(3):69.

5. Escobar-Morreale HF, Luque-Ramírez M, González F. Circulating inflammatory markers in polycystic ovary syndrome: a systematic review and metaanalysis. Fertil Steril. 2011 Mar 1;95(3):1048-1058.e1-2.

6. Aboeldalyl S, James C, Seyam E, Ibrahim EM, Shawki HED, Amer S. The Role of Chronic Inflammation in Polycystic Ovarian Syndrome-A Systematic Review and Meta-Analysis. Int J Mol Sci. 2021 Mar 8;22(5):2734.

7. Keskin Kurt R, Okyay AG, Hakverdi AU, Gungoren A, Dolapcioglu KS, Karateke A, et al. The effect of obesity on inflammatory markers in patients with PCOS: a BMI-matched case-control study. Arch Gynecol Obstet. 2014 Aug;290(2):315–9.

8. Ciaraldi TP, Aroda V, Mudaliar SR, Henry RR. Inflammatory cytokines and chemokines, skeletal muscle and polycystic ovary syndrome: effects of pioglitazone and metformin treatment. Metabolism. 2013 Nov;62(11):1587–96.

9. Barcellos CR, Rocha MP, Hayashida SA, Dantas WS, Dos Reis Vieira Yance V, Marcondes JA. Obesity, but not polycystic ovary syndrome, affects circulating markers of low-grade inflammation in young women without major cardiovascular risk factors. Hormones (Athens). 2015;14(2):251–7.

10. Shen SH, Shen SY, Liou TH, Hsu MI, Chang Y chin I, Cheng CY, et al. Obesity and inflammatory biomarkers in women with polycystic ovary syndrome. Eur J Obstet Gynecol Reprod Biol. 2015 Sep;192:66–71.

11. Peng Z, Sun Y, Lv X, Zhang H, Liu C, Dai S. Interleukin-6 Levels in Women with Polycystic Ovary Syndrome: A Systematic Review and Meta-Analysis. PLoS One. 2016;11(2):e0148531.

12. González F, Sreekumaran Nair K, Basal E, Bearson DM, Schimke JM, Blair HE. Induction of hyperandrogenism in lean reproductive-age women stimulates proatherogenic inflammation. Horm Metab Res. 2015 Jun;47(6):439–44.

13. Liu M, Gao J, Zhang Y, Li P, Wang H, Ren X, et al. Serum levels of TSP-1, NF-κB and TGF-β1 in polycystic ovarian syndrome (PCOS) patients in northern China suggest PCOS is associated with chronic inflammation. Clin Endocrinol (Oxf). 2015 Dec;83(6):913–22.

14. Zafari Zangeneh F, Naghizadeh MM, Masoumi M. Polycystic ovary syndrome and circulating inflammatory markers. Int J Reprod Biomed. 2017 Jun;15(6):375–82.

15. Alanbay I, Mutlu Ercan C, Coksuer H, Sakinci M, Karasahin KE, Ozturk O, et al. Neopterin: a promising marker for the inflammation in polycystic ovary syndrome. Gynecol Endocrinol. 2012 Nov;28(11):879–83.

16. Vasyukova E, Zaikova E, Kalinina O, Gorelova I, Pyanova I, Bogatyreva E, et al. Inflammatory and Anti-Inflammatory Parameters in PCOS Patients Depending on Body Mass Index: A Case-Control Study. Biomedicines. 2023 Oct 14;11(10):2791.

17. Arroyo P, Ho BS, Sau L, Kelley ST, Thackray VG. Letrozole treatment of pubertal female mice results in activational effects on reproduction, metabolism and the gut microbiome. PLoS One. 2019 Sep 30;14(9):e0223274.

18. Stener-Victorin E, Padmanabhan V, Walters KA, Campbell RE, Benrick A, Giacobini P, et al. Animal Models to Understand the Etiology and Pathophysiology of Polycystic Ovary Syndrome. Endocrine Reviews. 2020 Aug 1;41(4):bnaa010.

19. Esparza LA, Terasaka T, Lawson MA, Kauffman AS. Androgen Suppresses In Vivo and In Vitro LH Pulse Secretion and Neural Kiss1 and Tac2 Gene Expression in Female Mice. Endocrinology. 2020 Dec 1;161(12):bqaa191.

20. Coutinho EA, Esparza LA, Rodriguez J, Yang J, Schafer D, Kauffman AS. Targeted inhibition of kisspeptin neurons reverses hyperandrogenemia and abnormal hyperactive LH secretion in a preclinical mouse model of polycystic ovary syndrome. Hum Reprod. 2024 Sep 1;39(9):2089–103.

21. Day F, Karaderi T, Jones MR, Meun C, He C, Drong A, et al. Large-scale genome-wide meta-analysis of polycystic ovary syndrome suggests shared genetic architecture for different diagnosis criteria. PLoS Genet. 2018 Dec;14(12):e1007813.

22. Lim SS, Hutchison SK, Van Ryswyk E, Norman RJ, Teede HJ, Moran LJ. Lifestyle changes in women with polycystic ovary syndrome. Cochrane Database Syst Rev. 2019 Mar 28;3(3):CD007506.

23. Kokosar M, Benrick A, Perfilyev A, Fornes R, Nilsson E, Maliqueo M, et al. Epigenetic and Transcriptional Alterations in Human Adipose Tissue of Polycystic Ovary Syndrome. Sci Rep. 2016 Mar 15;6:22883.

24. Torres PJ, Skarra DV, Ho BS, Sau L, Anvar AR, Kelley ST, et al. Letrozole treatment of adult female mice results in a similar reproductive phenotype but distinct changes in metabolism and the gut microbiome compared to pubertal mice. BMC Microbiol. 2019 Mar 12;19(1):57.

25. Ruiz-Perez D, Guan H, Madhivanan P, Mathee K, Narasimhan G. So you think you can PLS-DA? BMC Bioinformatics. 2020/12/11 ed. 2020 Dec 9;21(Suppl 1):2.

26. Foo YZ, Nakagawa S, Rhodes G, Simmons LW. The effects of sex hormones on immune function: a meta-analysis. Biol Rev Camb Philos Soc. 2017 Feb;92(1):551–71.

27. Hensel JA, Khattar V, Ashton R, Ponnazhagan S. Characterization of immune cell subtypes in three commonly used mouse strains reveals gender and strain-specific variations. Laboratory Investigation. 2019 Jan 1;99(1):93–106.

28. Dapas M, Lin FTJ, Nadkarni GN, Sisk R, Legro RS, Urbanek M, et al. Distinct subtypes of polycystic ovary syndrome with novel genetic associations: An unsupervised, phenotypic clustering analysis. PLoS Med. 2020 Jun;17(6):e1003132.

29. GTEx Consortium. The Genotype-Tissue Expression (GTEx) project. Nat Genet. 2013 Jun;45(6):580–5.

30. Ascani A, Torstensson S, Risal S, Lu H, Eriksson G, Li C, et al. The role of B cells in immune cell activation in polycystic ovary syndrome. Suturina LV, Harper DM, Yanes Cardozo LL, editors. eLife. 2023 Jul 4;12:e86454.

31. Letrozole treatment of adult female mice results in a similar reproductive phenotype but distinct changes in metabolism and the gut microbiome compared to pubertal mice | BMC Microbiology | Full Text [Internet]. [cited 2024 Nov 25]. Available from: https://bmcmicrobiol.biomedcentral.com/articles/10.1186/s12866-019-1425-7

32. Clark NM, Podolski AJ, Brooks ED, Chizen DR, Pierson RA, Lehotay DC, et al. Prevalence of Polycystic Ovary Syndrome Phenotypes Using Updated Criteria for Polycystic Ovarian Morphology. Reprod Sci. 2014 Aug;21(8):1034–43.

33. Stener-Victorin E. Update on Animal Models of Polycystic Ovary Syndrome. Endocrinology. 2022 Dec 1;163(12):bqac164.

34. Johnson NP. Metformin use in women with polycystic ovary syndrome. Ann Transl Med. 2014 Jun;2(6):56.

35. Bharath LP, Agrawal M, McCambridge G, Nicholas DA, Hasturk H, Liu J, et al. Metformin Enhances Autophagy and Normalizes Mitochondrial Function to Alleviate Aging-Associated Inflammation. Cell Metab. 2020 Jul 7;32(1):44-55.e6.

36. Kristófi R, Eriksson JW. Metformin as an anti-inflammatory agent: a short review. 2021 Sep 1 [cited 2024 Nov 25]; Available from: https://joe.bioscientifica.com/view/journals/joe/251/2/JOE-21-0194.xml

37. Nicholas DA, Proctor EA, Agrawal M, Belkina AC, Van Nostrand SC, Panneerseelan-Bharath L, et al. Fatty Acid Metabolites Combine with Reduced β Oxidation to Activate Th17 Inflammation in Human Type 2 Diabetes. Cell Metab. 2019 Sep 3;30(3):447-461.e5.

38. Catterall T, Fynch S, Kay TWH, Thomas HE, Sutherland APR. IL-17F induces inflammation, dysfunction and cell death in mouse islets. Sci Rep. 2020 Aug 4;10(1):13077.

39. The metabolism-modulating activity of IL-17 signaling in health and disease | Journal of Experimental Medicine | Rockefeller University Press [Internet]. [cited 2023 Nov 2]. Available from: https://rupress.org/jem/article/218/5/e20202191/211951/The-metabolism-modulating-activity-of-IL-17

40. Velez LM, Abruzzese GA, Heber MF, Ferreira SR, Motta AB. Treatment with the synthetic PPARG ligand pioglitazone ameliorates early ovarian alterations induced by dehydroepiandrosterone in prepubertal rats. Pharmacol Rep. 2019 Feb;71(1):96–104.

41. Nelson ME, Madsen S, Cooke KC, Fritzen AM, Thorius IH, Masson SWC, et al. Systems-level analysis of insulin action in mouse strains provides insight into tissue- and pathway-specific interactions that drive insulin resistance. Cell Metab. 2022 Feb 1;34(2):227-239.e6.

Acknowledgments

We gratefully acknowledge Dr. Robert W. Williams and Dr. David E. James from the University of Tennessee for generously providing the mice used in this study. Their contribution was instrumental to the success of this research. I would like to express my sincere gratitude to my postdoctoral mentor Dr. Mark Lawson from the University of California San Diego for his unwavering support in development of the ideas presented in this work, particularly during the

preparation of my K99/R00 application. His guidance, mentorship, and encouragement were invaluable in completing this first independent project in my laboratory.

Funding:

National Institutes of Health grant R00 HD098330 (DN)
National Institutes of Health grant R00 HD098330 S1 (NU, DN)
NIH grant HD095412 (VGT)

Author contributions:

Conceptualization: NU, LV, MS, DN
Methodology: NU, LV, GDR, CN, KW, JA, AK, VT, BB, EW, AD, MS, DN
Investigation: NU, LV, GDR, CN, KW, JK, NN, JA, AK, VT, BB, EW
Visualization: NU, LV, GDR, CN KW, JK, NN
Supervision: NU, LV, CN, KW, VT, BB, EW, AD, MS, DN
Writing—original draft: NU, DN
Writing—review & editing: NU, LV, GDR, CN, KW, JK, NN, JA, AK, VT, BB, EW, AD, MS, DN

Competing interests: Authors declare that they have no competing interests.

Data and materials availability: All data are available in the main text or the supplementary materials

Figures and Tables

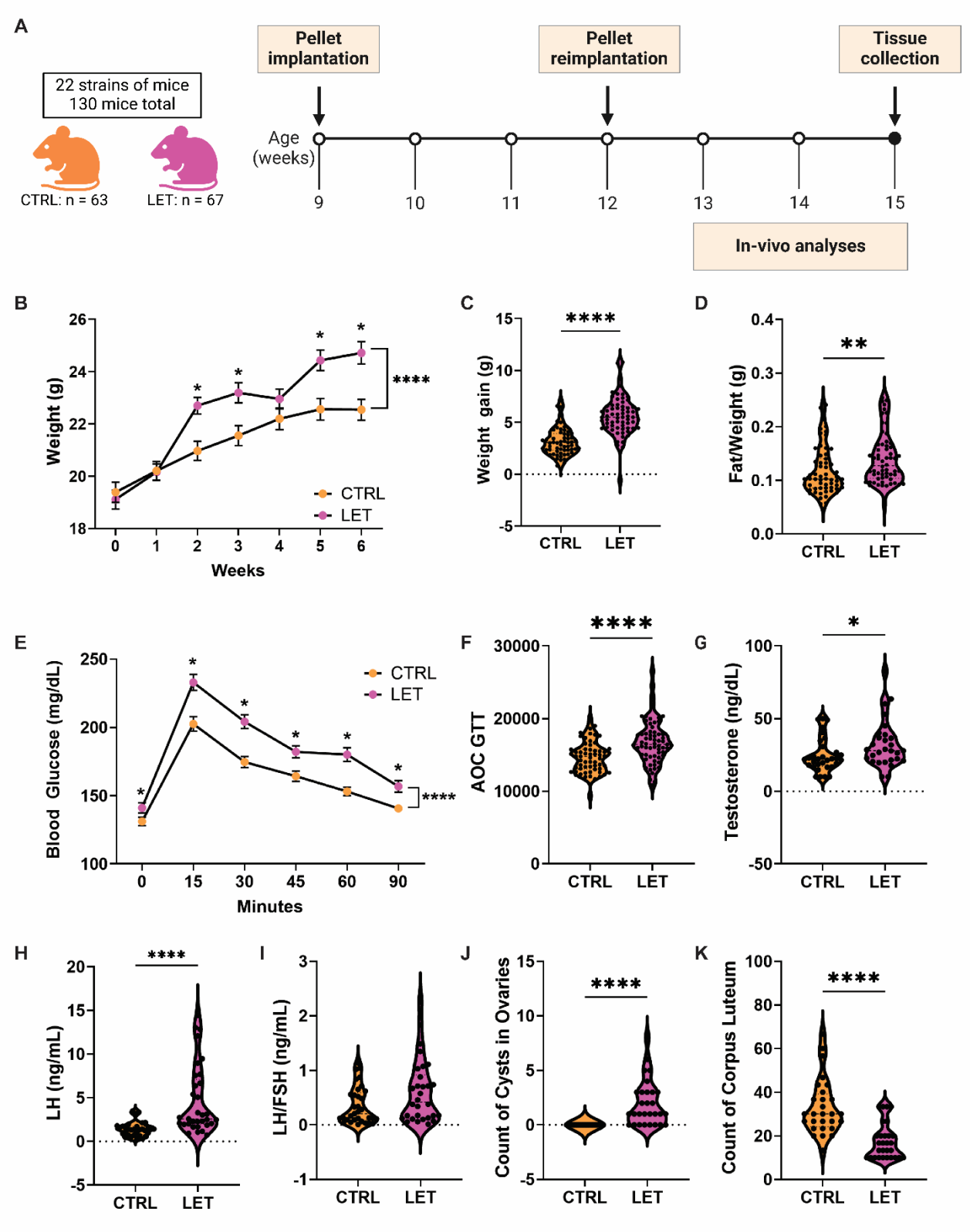

Fig. 1. Global Confirmation of PCOS-like symptoms in the LET-induced mouse model. (**A**) Timeline of letrozole or placebo pellet implantation at week 9 and 12. *In vivo* analyses (glucose tolerance testing, body composition, and estrous cycling) were measured between 13 to 15 weeks, and sac at 15 weeks included collection of spleen, inguinal lymph nodes and serum. (**B**)

Total body weight during the 6 weeks of treatment. (CTRL=63, LET=67). (**C**) Overall weight gain over a 6-week period (CTRL=63, LET=67). (**D**) Fat to total body weight ratio (CTRL=63, LET=67). (**E**) Blood glucose (mg/dL) in response to a glucose tolerance test (CTRL=61, LET=65). (**F**) Area of the curve derived from GTT measurements in (E) (CTRL=61, LET=65), (**G-I)** Serum hormone measurements: (**G**) Testosterone (ng/dL) (CTRL=32, LET=31), (**H**) luteinizing hormone, (**I**) ratio of luteinizing hormone to follicular-stimulating hormone (ng/mL) (CTRL=33, LET=30). (**J**) Count of cystic follicles per ovary (CTRL=27, LET=29). (**K**) Count of corpora lutea per ovary (CTRL=28, LET=29). Data are presented as mean ± SEM and analyzed with t-test for parametric data or Mann-Whitney test for nonparametric data. Significance was accepted at $p<0.05$ and is indicated with an *.

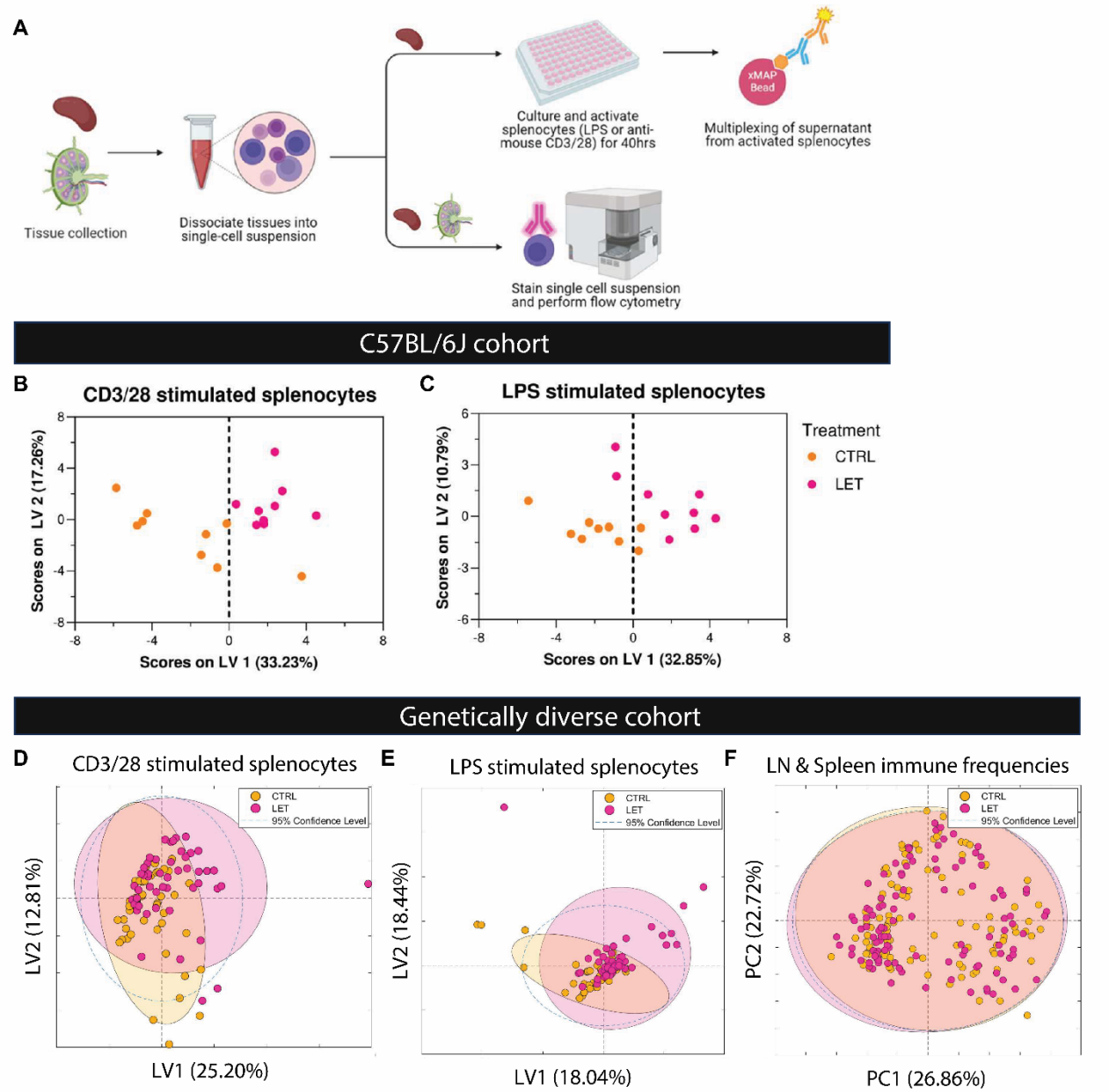

Fig. 2. LET-induced inflammation differences are overshadowed by genetic diversity. (**A**) Splenocytes from mice were dissociated into single cell suspensions and either activated for multiplexing of conditioned media or stained for flow cytometry, whereas lymph nodes were only dissociated and stained for flow cytometry. (**B-C**) PLSDA of 40 cytokines measured from the conditioned media of C57BL6 CTRL and LET splenocytes stimulated with anti-CD3/28 (cross validation class error average: 0.167) (B) or LPS (cross validation class error average: 0.278) (C). (**D-E**) PLSDA of 40 cytokines measured from the conditioned media of genetically diverse CTRL and LET splenocytes stimulated with anti-CD3/28 (cross validation class error average: 0.309) (D) or LPS (cross validation class error average: 0.225) (E). (**F**) PCA plot of genetically diverse CTRL and LET cohorts' immune frequencies by flow cytometry.

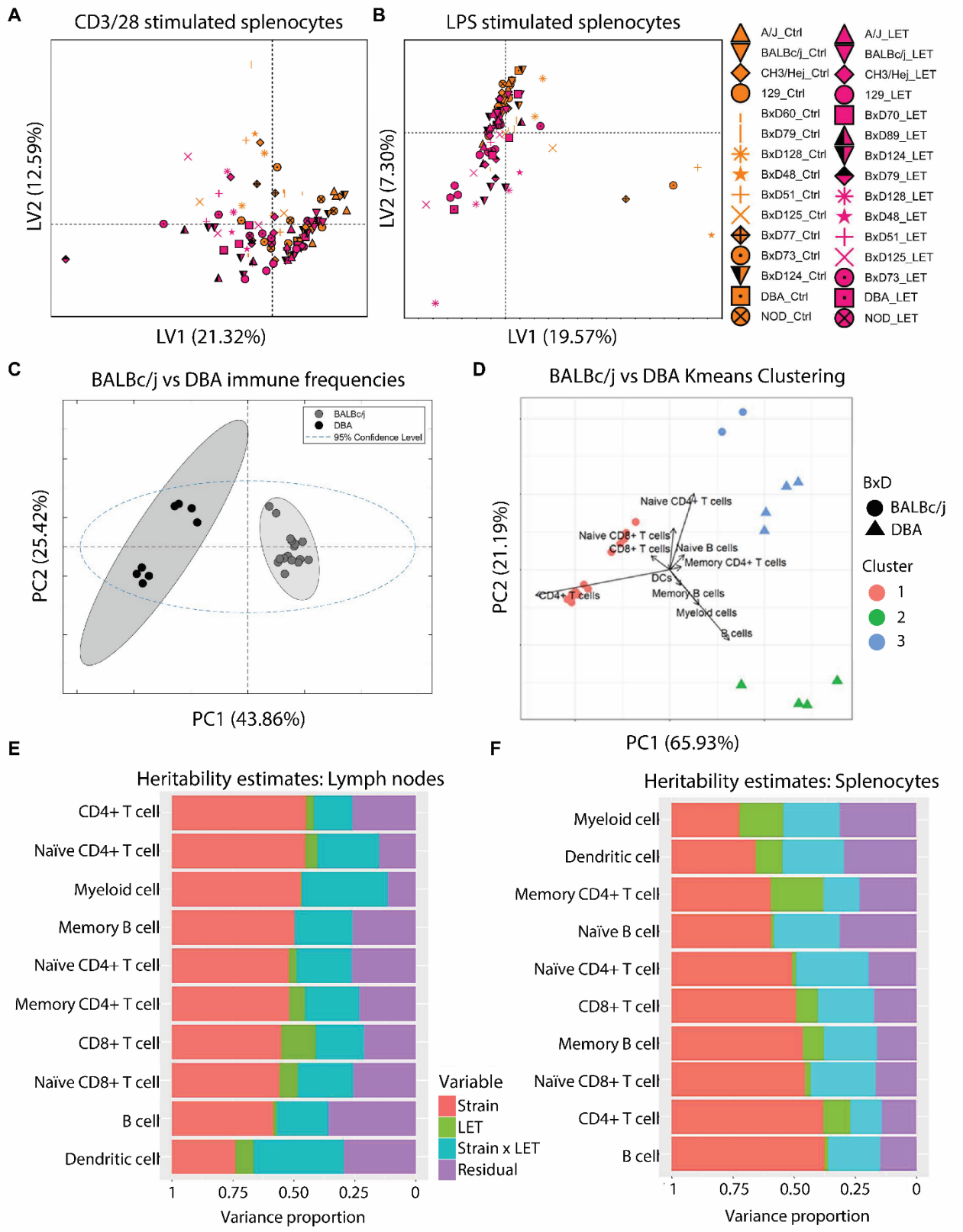

Fig. 3. Genetic diversity imposes shift in host immune profile, superseding LET-induction of PCOS symptoms.

(**A-B**) Splenocytes from the genetically diverse cohort of mice were dissociated into single cell suspensions and either stimulated with anti-CD3/28 (cross validation class error average: 0.351) (A) or LPS (cross validation class error average: 0.323) (B). PLSDA analysis was performed and annotated by strain. (**C**) PCA plot of immune frequencies via flow cytometry from BALBc/j and

DBA strains. (**D**) PCA plot with K means clustering projection of immune frequencies via flow cytometry from BALBc/j and DBA strains. (**E-F**) Heritability estimates of lymph node (E) or splenocyte (F) immune frequencies from genetically diverse cohorts via flow cytometry.

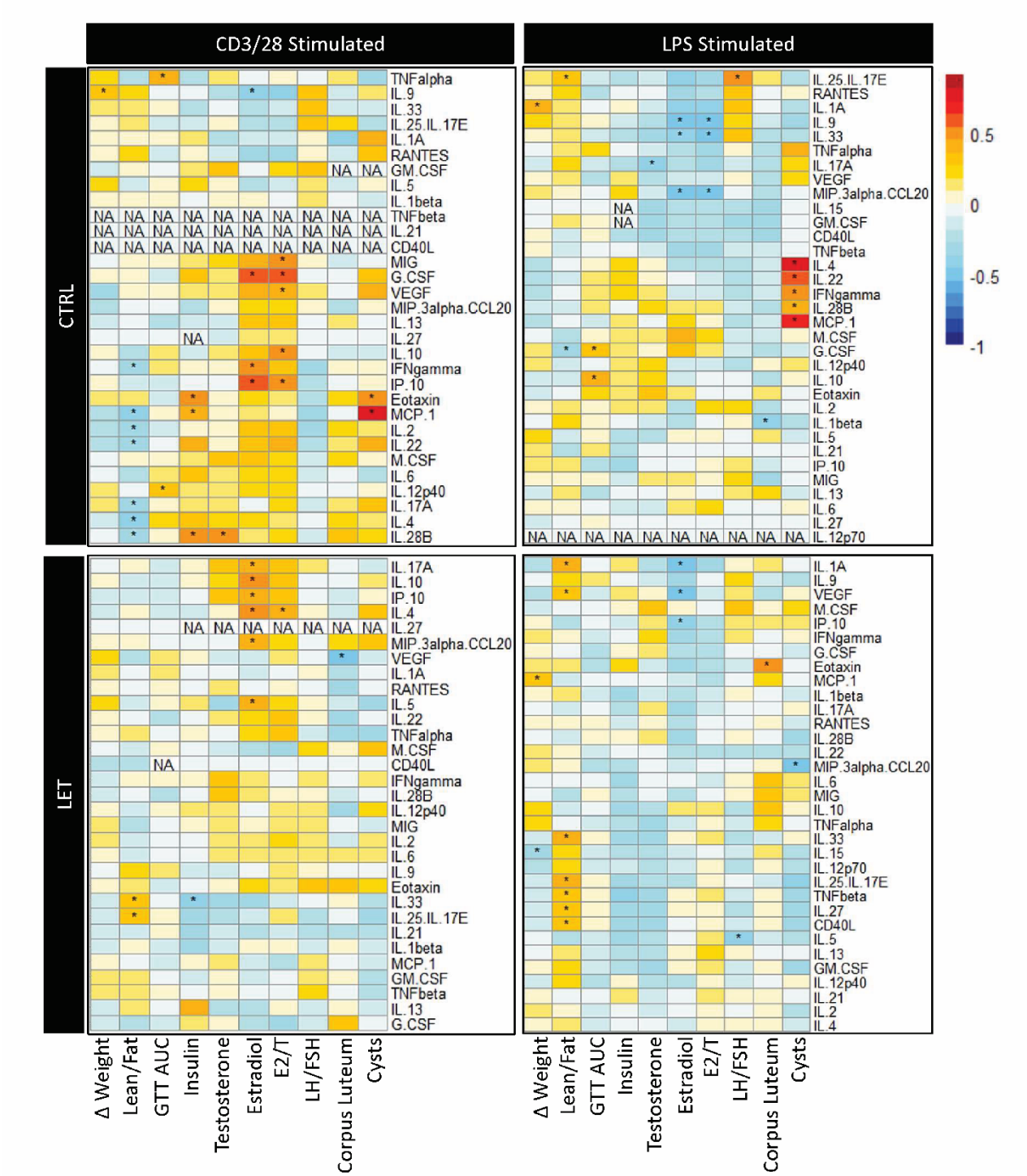

Fig. 4. T cell derived cytokines correlate with LET induced PCOS like symptoms. Heatmap depicting correlative relationships between cytokine concentration and PCOS-like phenotypes. Splenocytes from the genetically diverse CTRL and LET cohorts were stimulated with anti-CD3/28 or LPS. Conditioned media was assayed for cytokines by multiplex analysis. Red denotes strong, positive correlation. White denotes no correlation. Blue denotes strong, negative correlation. Asterisk (*) denotes statistically significant correlations.

Table 1. Strains of mice subclassified by PCOS phenotypes.

Genetically diverse strains of LET cohort were categorized as similar to subtype A, B, C or D based on hyperandrogenism status, presence of oligo-anovulation and polycystic ovarian morphology. Strains were classified as hyperandrogenic if a strain's LET cohort had an average testosterone that was 1.5-fold change or higher compared to the strain's CTRL cohort's average. Oligo-anovulation was classified if the strain's LET cohort average cycling was less than the strain's CTRL cohort average cycling. A positive polycystic ovarian morphology status was deemed if the strain's LET cohort had a statistically higher average count of cysts and a negative 1.5 fold change or higher of corpus luteum compared to the strain's CTRL cohort. For missing values or underpowered strains, the strains were deemed uncategorized. Genetically diverse strains of the LET cohort were then categorized as high metabolic dysfunction if previously categorized as A or B subtype, and low metabolic dysfunction if previously categorized as C or D subtype.

Strain	**Hyperandrogenism** >=1.5FC	**Estrous cyclicity** LET < CTRL	**PCOM** LET > CTRL = high cysts and 1.5FC CL	**Subtype**	**Metabolic Dysfunction**
A/J	✓	✓	**x**	B	High
BALBc/j	**x**	✓	**x**	Uncategorized	Uncategorized
BxD 124	✓	✓	✓	A	High
BxD 125	✓	✓	**x**	B	High
BxD 128	**x**	✓	**x**	Uncategorized	Uncategorized
BxD 129	✓	✓	✓	A	High
BxD 44	---	---	---	Uncategorized	Uncategorized
BxD 48	✓	**x**	✓	C	Low
BxD 51	**x**	**x**	**x**	Uncategorized	Uncategorized
BxD 60	✓	✓	✓	A	High
BxD 70	---	---	---	Uncategorized	Uncategorized
BxD 71	---	---	---	Uncategorized	Uncategorized
BxD 73	**x**	✓	**x**	Uncategorized	Uncategorized
BxD 75	**x**	✓	---	Uncategorized	Uncategorized
BxD 77	**x**	✓	✓	D	Low
BxD 78	---	---	---	Uncategorized	Uncategorized
BxD 79	✓	**x**	✓	C	Low
BxD 89	---	---	---	Uncategorized	Uncategorized
CH3/Hej	✓	✓	✓	A	High
DBA	✓	✓	✓	A	High
NOD	✓	✓	✓	A	High

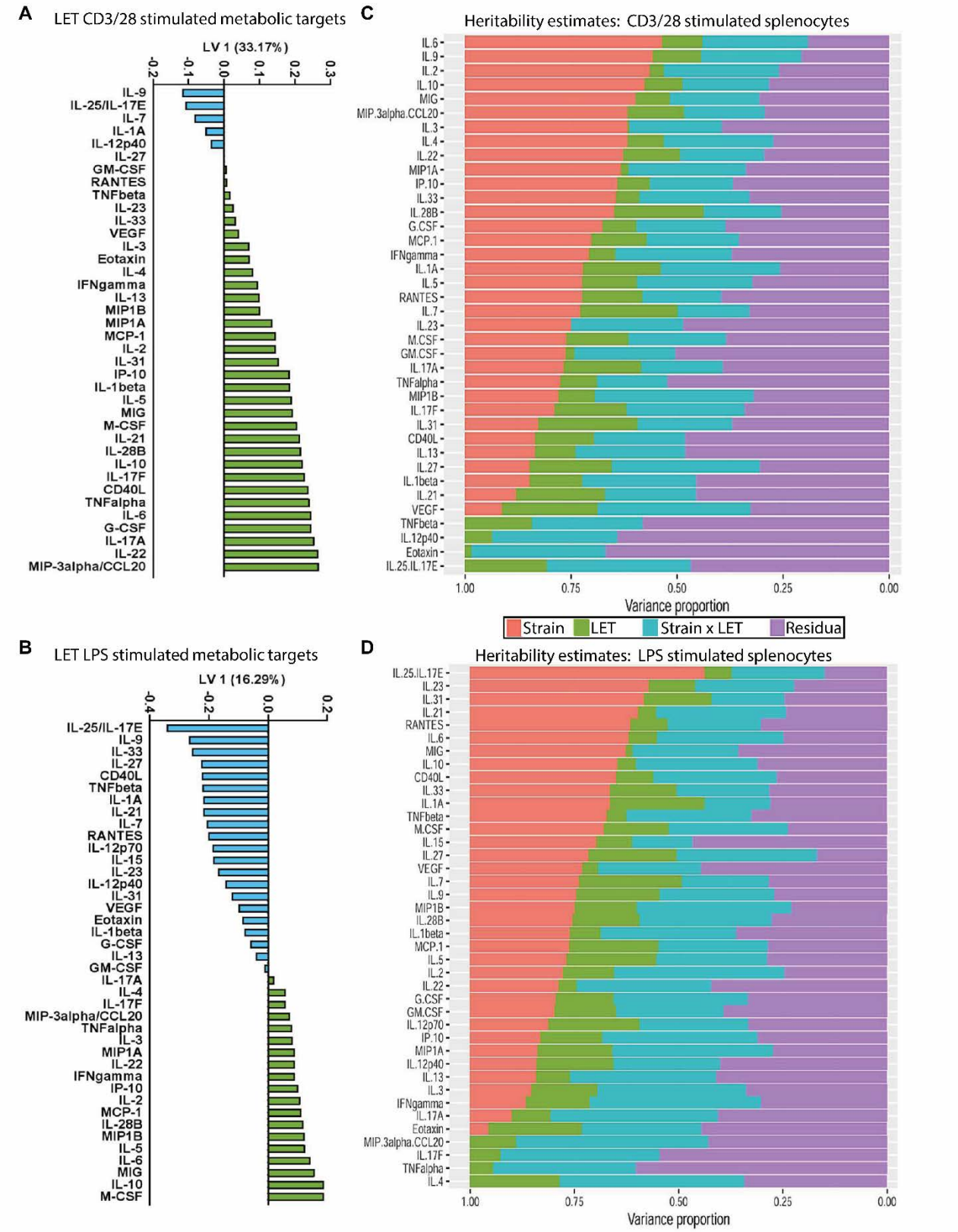

Fig. 5. T cell derived cytokines differentiate metabolic status and are LET specific. (**A-B**) LV1 loadings of 40 cytokines measured from the conditioned media of C57BL6 CTRL and LET splenocytes stimulated with anti-CD3/28 (A) or LPS (B). Cytokines with negative values are important for differentiating high metabolic dysfunction, while cytokines with positive values differentiate low metabolic dysfunction. (**C-D**) Heritability estimates across the genetically

825 diverse cohort of cytokine concentrations from the conditioned media of splenocytes stimulated
826 with anti-CD3/28 (C) or LPS (D).
827
828
829
830

831 **Table 2. PCOS associated clinical parameters of women with no PCOS diagnosis (n = 5), or**
832 **with PCOS diagnosis (n = 15).**
833

	No PCOS Dx	PCOS	P-value	Significance
Age	30.4 ± 3.91	25.93 ± 3.69	0.0604	NS
BMI	25.64 ± 6.64	27.25 ± 4.91	0.4973	NS
Menses/year	12 ± 0	7.07 ± 2.52	<0.0001	****
R ovarian volume	6.88 ± 3.12	14.19 ± 4.48	0.0035	**
L ovarian volume	7.96 ± 3.15	13.66 ± 6.37	0.0328	*
Testosterone	0.32 ± 0.10	0.75 ± 0.26	0.0003	***
SHBG	66.16 ± 30.30	43.55 ± 25.89	0.1186	NS
DHEAS	4.59 ± 1.68	9.70 ± 4.91	0.0025	**
LH	7.44 ± 2.54	11.46 ± 6.78	0.3486	NS
FSH	6.72 ± 2.18	5.84 ± 1.99	0.5531	NS
E2	57.84 ± 15.45	60.75 ± 24.22	0.866	NS
PRL	21.01 ± 4.81	20.99 ± 5.59	0.9466	NS
Cholesterol	139.86 ± 39.86	160.94 ± 29.53	0.3486	NS
Triglycerides	83.60 ± 36.91	97.95 ± 45.53	0.0178	*
HDL	50.70 ± 12.50	54.75 ± 10.95	0.0093	**
LDL	72.46 ± 35.33	86.64 ± 25.81	0.2504	NS
TSH	1.79 ± 0.45	1.23 ± 0.60	0.0003	***

834
835

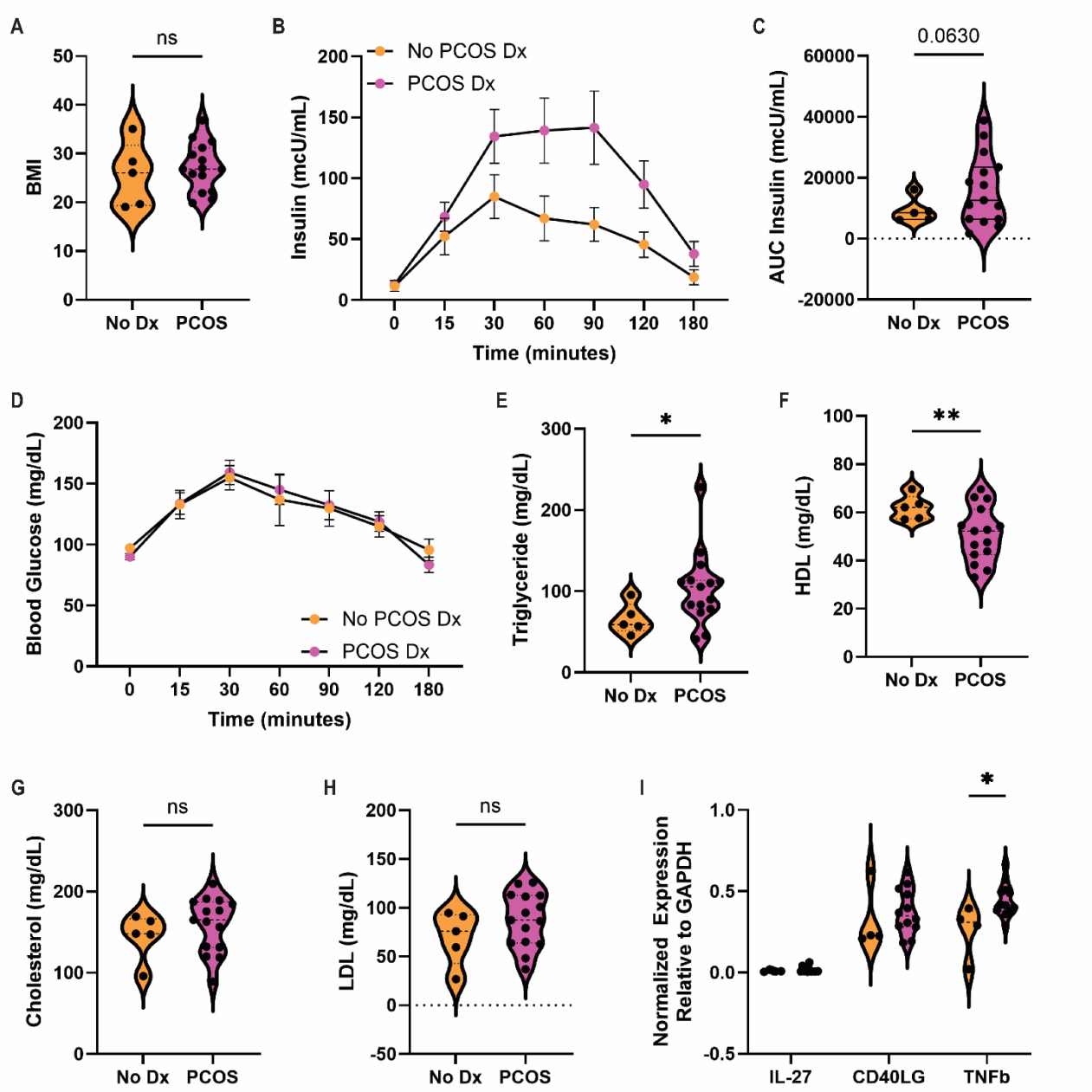

Fig. 6. TNF-β mRNA expression is higher in PBMCs of women with PCOS.
(**A-H**) Clinical parameters of the PCOS cohort. (A) Body mass index, BMI, (B) Insulin response, (C) Area under the curve of insulin response from (B), (D) Glucose tolerance test, (E) total triglycerides, (F) total high density lipoproteins, (G) total cholesterol, and (H) total low density lipoproteins measured in women with no PCOS diagnosis (n = 5) and with PCOS diagnosis (n = 16). (**I**) qPCR of mRNA expression of pro-inflammatory cytokines (IL-27, CD40LG, TNF-β) measured in PBMCs of women with no PCOS diagnosis (n = 4) and with PCOS diagnosis (n = 12). Data are presented as mean +/= SEM and analyzed by student's t-Test with significance accepted at $p<0.05$.

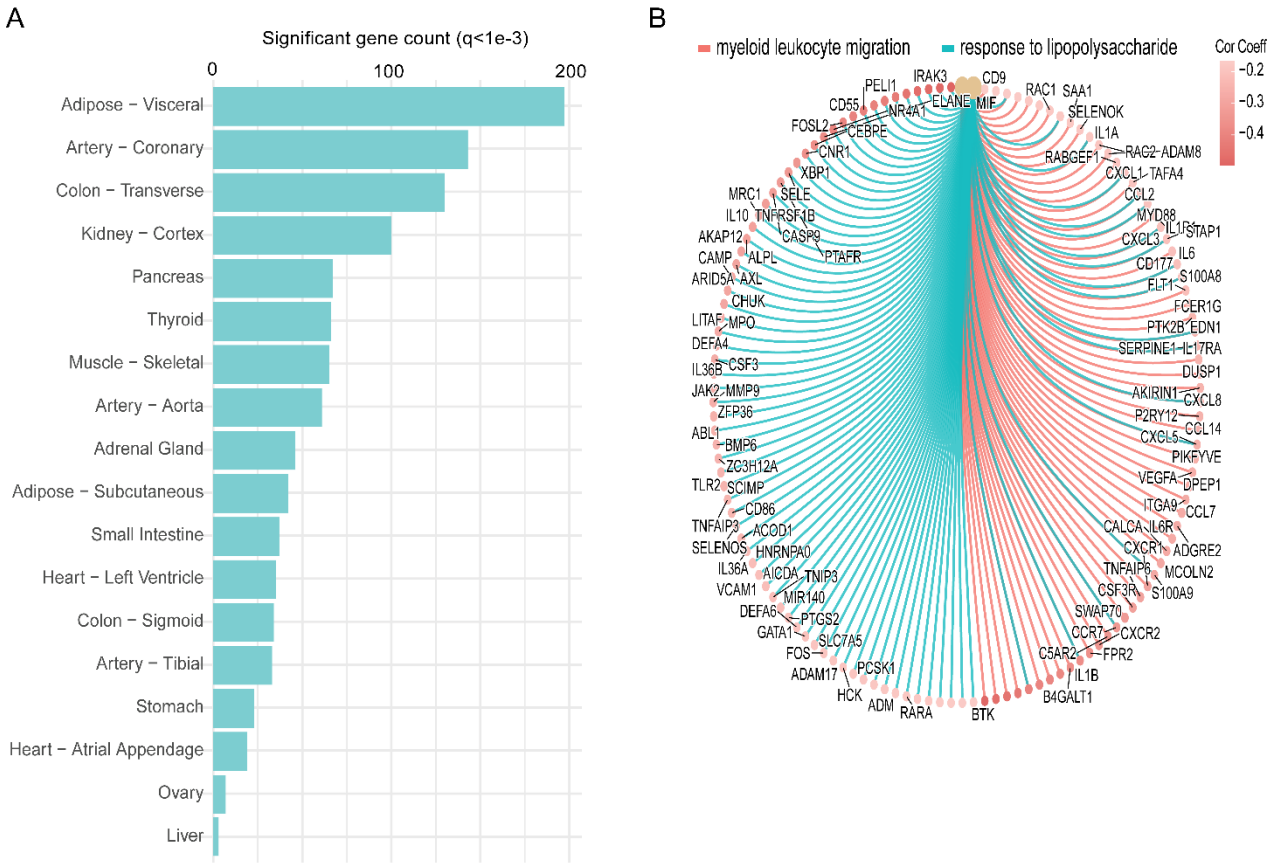

Figure 7. Human Genetic variation implicates TNF-β in cross tissue regulation of adipose inflammation.

(**A**) The number of genes per organ that is significantly correlated with *LTA* expression in pre-menopausal human female spleen. (**B**) A cnet graph showing the *LTA*-correlated adipose genes from the top significantly correlated pathways “myeloid leukocyte migration” and “response to LPS”.

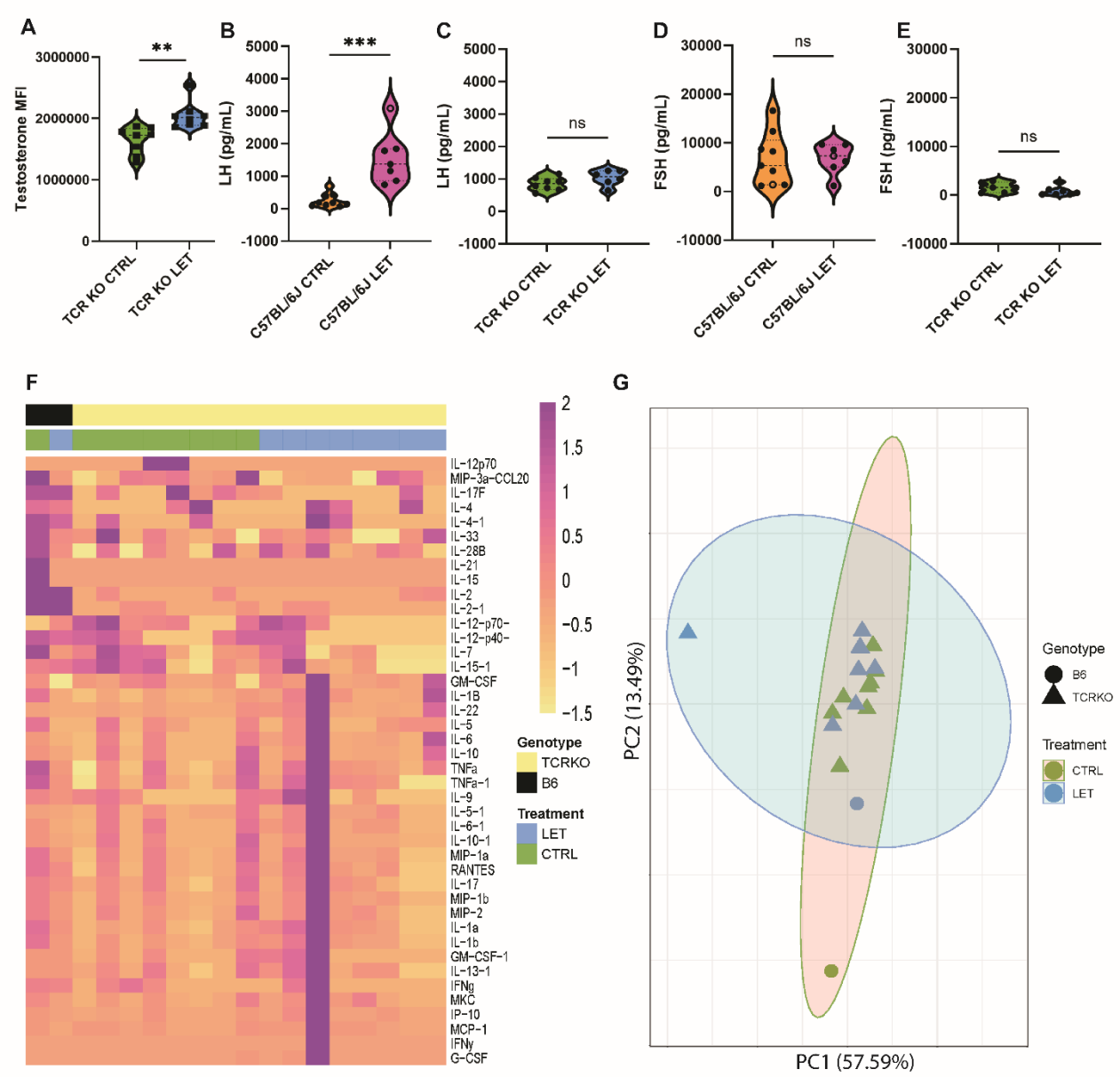

Fig. 8. The PCOS reproductive phenotype and cytokine profile is dependent on T cells. (**A**) Mean Fluorescence Intensity (MFI) of pre-extracted serum testosterone from C57BL6 TCRαKO serum after weeks of Placebo or LET exposure. Testosterone was measured via Luminex Multiplex. (**B-E**) Serum LH (B-C) and FSH (D-E) in control (Placebo) and LET-treated C57BL6 mice after 5 weeks of LET exposure starting at 9 weeks of age. (**A and C**) C57BL6 wildtype mice. Filled circles are data from Torres et al. 2019 and open circles are data from sentinel mice. (**B and D)** C57BL6 TCRαKO. Data are presented as mean +/= SEM and analyzed by student's t-Test with significance accepted at $p<0.05$. (**F**) Heatmap depicting z-scored cytokine concentration. Splenocytes from the C57BL6 TCRαKO CTRL and LET cohort along with control and LET-treated sentinel mice were stimulated with LPS. Conditioned media was assayed for cytokines by multiplex analysis. (**G**) Principal component analysis of cytokine data from (F).

Supplementary Materials

Figs. S1 to S7

Tables S1 to S2

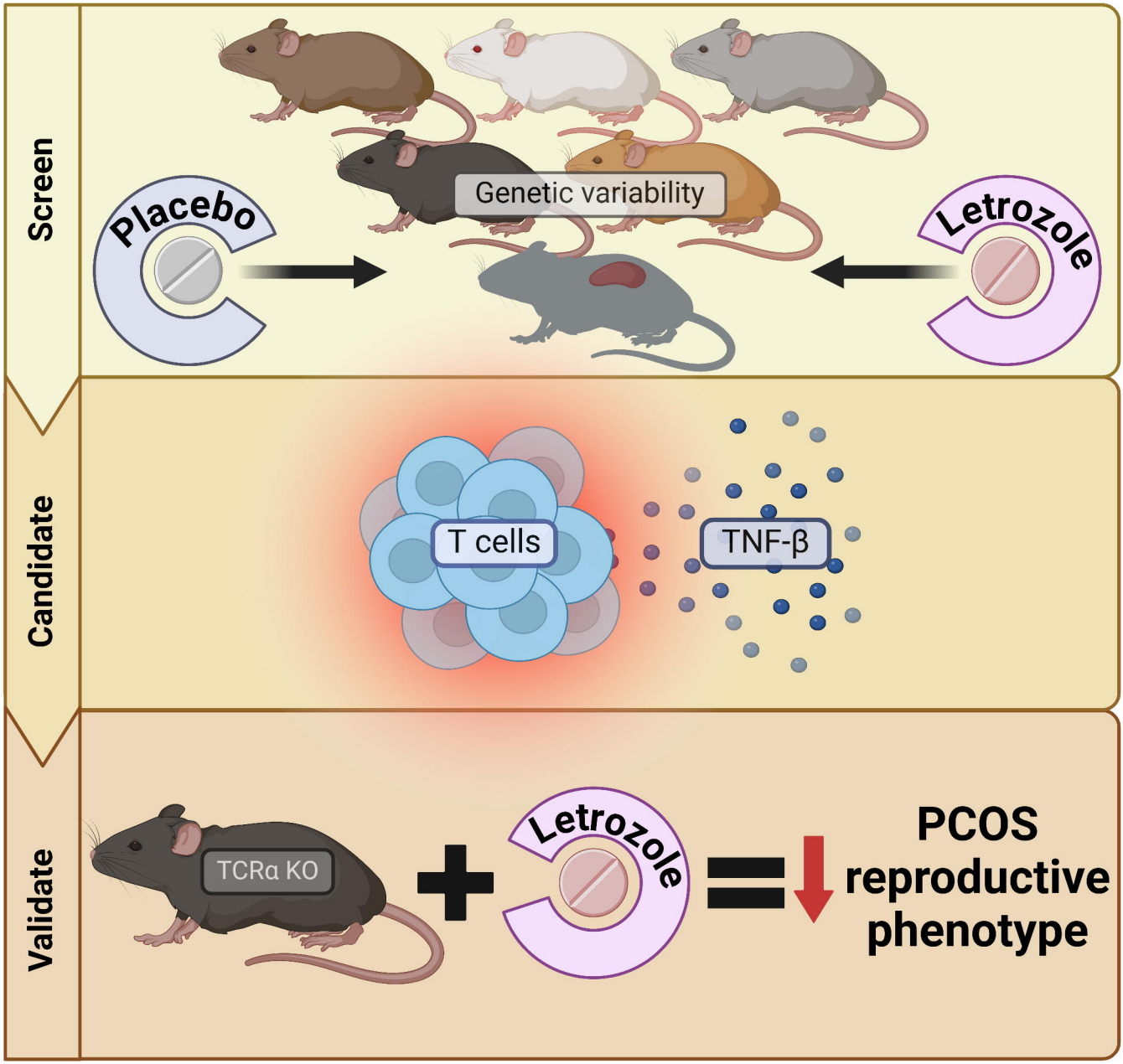
Screen
Placebo
Genetic variability
Letrozole
Candidate
T cells
TNF-β
Validate
TCRα KO
Letrozole
PCOS
reproductive
phenotype